Surface Science 677 (2018) 213–218

Contents lists available at ScienceDirect

Surface Science

journal homepage: www.elsevier.com/locate/susc

Scanning tunneling microscopy and photoemission studies of self-organised Ag nanostructures on the N-modified Cu(001) surface

Paola Finetti[a,c], Luisa Ferrari[b], Sergio D'Addato[*,c,d]

[a] Elettra-Sincrotrone Trieste S.C.p.A., 34149, Trieste, Italy
[b] CNR-ISM, Via Fosso del Cavaliere 100, 00133, Roma, Italy
[c] Dipartimento FIM, Università di Modena e Reggio Emilia, via G. Campi 213/a, 41125, Modena, Italy
[d] CNR, Istituto Nanoscienze, via G. Campi 213/a, 41125, Modena, Italy

ARTICLE INFO

Keywords:
self-assembling
Ag
c(2 × 2)-N/Cu(001) surface
Quantum well states
STM
ARPES

ABSTRACT

There has been a strong interest in methods of creating nanometer scale structures and in particular forming one- and two-dimensional electron confinement structures. Self-organisation has been recognised as a promising way for growing large nanostructure domains with sufficiently regular size and spacing as required for the observation of quantum well states. We investigated the electronic properties and the morphology of Ag nanostructures on c(2 × 2)-N/Cu(001) surface. This system is an example of epitaxial growth confined on nanoscale regions due to the occurrence of an adsorbate induced reconstruction. Using a combination of Scanning Tunneling Microscopy and Angle Resolved Photoemission Spectroscopy techniques we were able to determine the morphology and the growth mode of Ag on N-modified Cu(001) surface and the occurrence of quantum size effects in the electron properties of Ag nanostripes and nanoislands, evidenced in the observation of quantum well states.

1. Introduction

The bottom-up approach in the design and realization of nanostructure assemblies is a well-established method in nanoscience, and still it presents some fascinating aspects: in particular, fabrication of 2-D self-organized patterns and their use for creating regular assemblies of dots, wires and stripes is one of the most interesting phenomena in physics and chemistry, also for technological application [1-12]. In particular, adsorption of atomic nitrogen on the Cu(001) surface is a very good example of self-organisation [13,14]: at N-coverage Θ_N below saturation (saturation occurs at $\Theta_N = 0.5$ ML) the adsorption results in fact in the formation of regular arrays of square N islands with c(2 × 2) internal periodicity that run parallel to the ⟨100⟩ azimuth. The size of the square islands does not depend on the N-coverage and is equal to about 5 × 5 nm^2. The spacing between islands along the array is given by one line of Cu atoms, while the spacing between the arrays is inversely proportional to the N coverage. This peculiar arrangement of the adsorbates leaves stripe-shaped domains of clean Cu having a regular width. It was found that this periodic arrangement is caused by difference of surface stress in the clean and nitrided domains, and their competition with the domain boundary energy [15,16]. The regular island morphology can be monitored with Scanning Tunneling Microscopy (STM) [13,14], with Low Energy Electron Diffraction (LEED) [17,18] and Surface X-ray Diffraction (SXRD), in the last two cases by directly observing four-fold satellite peaks which appears around the (10) diffraction spots [16,19]. When the N coverage reaches a value $\Theta_N = 0.5$ ML, the square islands coalesce, with formation of an almost continuous N layer, with some interruptions caused by trenches parallel to ⟨110⟩ directions, which have a width of few nanometers and a height of a single atomic layer [13,14]. More recently, ribbon-like nanopatterns were obtained in vicinal regions toward ⟨100⟩ directions, with formation of N islands of rectangular shapes [20]. The N-modified Cu surface exhibits also strong reactivity to atomic H exposure, with formation of NH species at the surface and, by increasing the amount of H dosage, with formation and desorption of ammonia [21].

STM experiments found out that when transition metals such as Cu, Fe, Ni, Ag, Co, Au are deposited on the N-modified Cu(001) surface, epitaxial growth at its initial stages occurs preferentially on the clean Cu stripes [1,22-27], rather than on the N-covered parts of the surface. Therefore metal particles and stripes can be grown on the clean Cu areas, but the evolution of the growth with the metal coverage depends strongly on the particular metal used. For instance, the origin of preferential growth of Fe islands on bare Cu(001) areas was assigned to inclusion of Fe atoms at very low Fe coverage stage. These inclusions

* Corresponding author at: FIM, Università di Modena e Reggio Emilia, Via G. Campi 213/a, 41125 Modena, Italy.
E-mail address: sergio.daddato@unimore.it (S. D'Addato).

https://doi.org/10.1016/j.susc.2018.07.009
Received 6 June 2018; Received in revised form 16 July 2018; Accepted 17 July 2018
Available online 19 July 2018
0039-6028/

worked as centers of nucleation for the growth of 2D Fe islands on top of the Cu bare surface areas. After the bare Cu areas are completely covered, the Fe nanostructured films extend over the N-covered patches. X-ray Absorption Fine Structures (XAFS) studies confirmed the preferential growth of Fe islands on the bare Cu surfaces for $\Theta_N < 0.5$ ML, with Fe arranged in fcc lattice [28-30], and with the presence of some disorder in the islands, with inhomogeneous lattice distortion caused by tetragonal expansion and the presence of surface atoms arranged in nano-martensitic phase. When Fe is adsorbed on saturated c(2 × 2)-N surface, XAFS data analysis are compatible with a geometry where the Fe atoms substitute the Cu atoms underneath the N layer. Fe-Cu bond length values are instead typical of Fe in a fcc site [30]. SXRD experiments on the same system were also performed; Crystal Truncation Rods (CTR) analysis substantially confirmed the results of XAFS [19]. Co and Fe nanostructured films on N-modified Cu (001) exhibited also interesting magnetic properties, as revealed by magneto-optical Kerr effect [31], dichroism in photoemission [32] and absorption [33].

Ag nanostructured films on N-modified Cu surfaces were investigated, for low Ag coverage, with STM, showing the possibility of creating single crystal Ag nanowires on sub-saturated c(2 × 2)-N/Cu (001). The Ag nanowires formed on the bare Cu areas between the arrays of N islands and are therefore aligned along the < 100 > direction, up to 4 atomic layers thick [1,34]. The growth of Ag on the bare Cu areas followed the same evolution as the formation of Ag ultrathin films on clean Cu(001), with formation for low coverage of a c (10 × 2) superstructure, followed by a simple pseudoexagonal overlayer structure [35].

On the other hand, the effect of reduced dimensionality on the electron properties of Ag ultrathin films shown itself in a spectacular way by the onset of quantum well states, observed with Angle Resolved Photoemission Spectroscopy (ARPES) and due essentially to the confinement of Ag electrons by the film-vacuum and film-substrate interface. The films were grown on a variety of single crystal surfaces, either metals or semiconductors [36-44]. Aim of this work is to investigate the effect of the N-induced nanopatterning of Cu(001) on the Ag electronic states, in particular, the effect of lateral confinement induced by N surface nanostructuring on the QW. The present study follows the morphology of the growth of Ag on the N modified Cu(001) surface by means of STM from the very early stages and up to 8 ML. The electronic structure of the Ag overlayer is studied by means of angular integrated photoemission spectroscopy (PES) and ARPES.

2. Experimental

The Cu(001) surface was cleaned by cycles of Ar sputtering at 1 keV ion impact energy and annealing at 550 °C. The cleanliness of the surface thus obtained was checked by LEED and PES and by STM where applicable. The N overlayer was prepared by sputtering the Cu(001) surface with N_2 at medium ion impact energy (500 eV) until the accumulated charge on the sample (i.e. the product of the sample drain current and the sputtering time) was of the order of 90 μC. Cross-check also with previous STM observations shown that with this dosage the N precoverage is about 0.25 ML. The N_2 sputtering was followed by prolonged annealing (at least one hour) of the sample at 350 °C. This procedure resulted in a sharp LEED and large domains of N islands arrays as revealed also by STM. The photoemission experiments were carried on VUV-Photoemission and APE beamlines, both at the synchrotron radiation laboratory of Elettra, Trieste, during two different runs. STM data were acquired in a chamber connected with the APE endstation.

The N-Cu(001) surface prior to Ag deposition was characterized by means of low energy electron diffraction (LEED) every time. This technique allows to detect the formation of long arrays of c(2 × 2)-N islands due to the presence of extra diffraction spots to be attributed to long periodic structures such as the islands arrays. [13,14,22]. Ag was evaporated at room temperature from an Ag bead heated in an alumina crucible and no annealing procedure was applied to the overlayer. The amount of deposited Ag was determined by means of a calibrated quartz microbalance. Two Cu(001) crystals were employed for the ARPES and STM experiments and identical Ag evaporators were mounted at the same distance from the sample in all the experimental chambers to ensure the same amount of deposited Ag observed in STM and (AR)PES experiments. ARPES data were acquired with $k_{\parallel}$ varying along the ⟨100⟩ and ⟨110⟩ azimuthal direction.

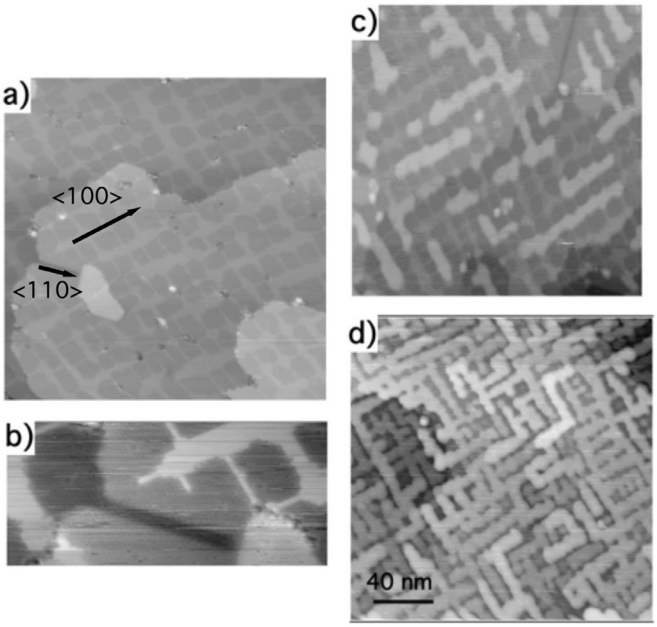

Fig. 1. (a) and (b) 0.25 ML of c(2 × 2)-N/Cu(001). The N covered parts appear as depressions. The N islands are about 5 × 5 nm^2. (c) 0.25 ML of c(2 × 2)-N/Cu(001) plus 0.1 ML of Ag (showing as striped protrusions). (d) 0.25 ML of c (2 × 2)-N/Cu(001) and 0.5 ML of Ag. Small, but high and round protrusions appearing occasionally on 1 (a), (c) and (d) which are due to the tip.

3. Results and discussion

3.1. STM results

Fig. 1a-b shows some examples of STM images from the N precovered surface. Our images are similar to the ones obtained in previous studies in which the N growth mode has been described accurately [13,14,22] and here we report some results for the sake of clarity. The N islands appear as depressions in the image. From Fig. 1(a) it can be estimated that the N coverage is about 0.25 ML, i.e. about 50% of the initial surface is made of two domains of c(2 × 2)-N islands arrays and by domains of clean unreconstructed Cu(001) stripes running along the ⟨100⟩ azimuthal direction.. Fig. 1b shows faceting of the island at the island corners and the occasional coalescence of N islands at the junction between domains of N islands with edges terminating along the ⟨110⟩ azimuthal direction. This peculiarity in the N overlayer is rarely found and it is reported here as an example.

Fig. 1(c) and (d) and Fig. 2(a)–(e) report the growth of Ag on the N modified Cu surface, from the very early stage (0.1 ML of Ag) up to coverage values corresponding to a volume of 8 flat Ag monolayers on Cu(001). The growth of Ag on bare Cu(001) has been extensively studied with a number of techniques. In summary, at a thickness of up to 1 ML, the Cu and Ag lattice mismatch determines a growth of Ag in the shape of a quasi hexagonal c(2 × 10) structure [34,35,45,46]. Note that room temperature Cu(001)- Ag alloying, confined to the 2D surface, was predicted for very low Ag coverages ($\Theta_{Ag} < 0.13$ ML) [47]. From the data shown in Fig. 2(c) we cannot give evidence of this process. At

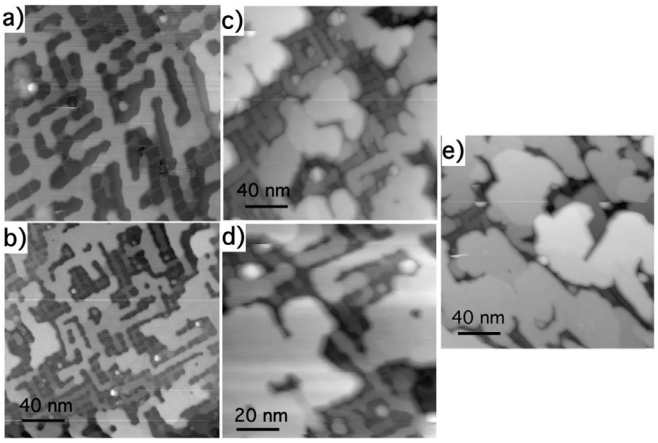

Fig. 2. In all the figures the Cu(001) surface was modified by the adsorption of 0.25 ML of c(2 × 2)-N. (a) 1 ML of Ag. (b) 2 ML of Ag. (c) and (d) 4 ML of Ag. (e) 8 ML of Ag. In all images, sharp round shaped protrusions are tip effects.

higher thickness the Ag overlayer grows as unreconstructed Ag(111) [34, 46]. Also the early growth (up to 2 ML) of Ag on N modified Cu (001) was reported in the past by STM [1,33]. It was shown [34] that the growth of Ag in this case proceeds in the same guise as on the clean Cu(001) surface, i.e., with a c(2 × 10) periodicity for the first layer of Ag growing on clean Cu and forming an unreconstructed Ag(111) layer for Ag stripes of higher thickness. In this paper we consider much higher coverage values than previously reported and the whole sequence of Ag overlayers is here discussed. Two types of Ag growth modes can be identified: for $0 < \Theta_{Ag} < 2$ ML the growth is entirely confined on the Cu stripes (see Fig. 1(c),(d) and Fig. 2(a)) and proceeds predominantly in a layer by layer fashion. In particular, at the Ag coverage of 0.5 ML all the Cu stripes are covered by Ag with a thickness of 1 atomic layer (the Ag(111) step size is 2.36 Å) and occasionally double layered Ag islands can be observed (see Fig. 1(d)). This finding is consistent with some marginal error in the determination of the N pre-coverage and with a small error in the calibration of the deposited Ag. The LEED observations confirm the c(2 × 10) periodicity of the Ag overlayer at this Ag coverage.

At about 1 ML of deposited Ag thickness, the Ag forms predominantly a double layer (see Fig. 2(a), but the height of the striped Ag domains can reach up to 6 (see Fig. 3(a)) atomic layers and the LEED shows the presence of Ag(111) domains. At about 2 ML we observed the onset of islands formation (see Fig 2(b)). The growth of these 2D islands is both lateral and vertical, and the LEED shows a pattern consistent with an Ag(111) films. Above 2 ML the lateral growth becomes predominant, with heights reaching 7 atomic layers at about 4 ML of deposited Ag volume (see Fig. 3(b)), although non-negligible areas of N-covered Cu could still be observed with STM even for the highest Ag nominal thickness (8 ML). In this case the islands can reach a height of 10 monolayers (see Fig. 3(c)). The Ag islands display an atomically flat top and peculiar faceting induced by the N-modified substrate. It can also be noticed that their thickness tends to be rather uniform across the surface. This can be seen both from the STM images and from the line profiles, shown on Fig. 3c. Note that the profiles were acquired in regions where the Ag coverage is more variable. Also, in the profile at 8 ML there is no safe assignment of the baseline to an Ag free area. The 10 ML height of the highest island is then an estimate.

In summary, we observed a layer by layer type of growth throughout the Ag coverage range reported in this study, despite the non uniform substrate conformation. From our STM data we could not find clear evidence of displacement of N atoms upon Ag growth. However, N segregation was observed previously on Co nanostructured films grown on the same surface, as a result of strain induced by the formation of Co nano-islands [48]. It is quite possible that the flatness

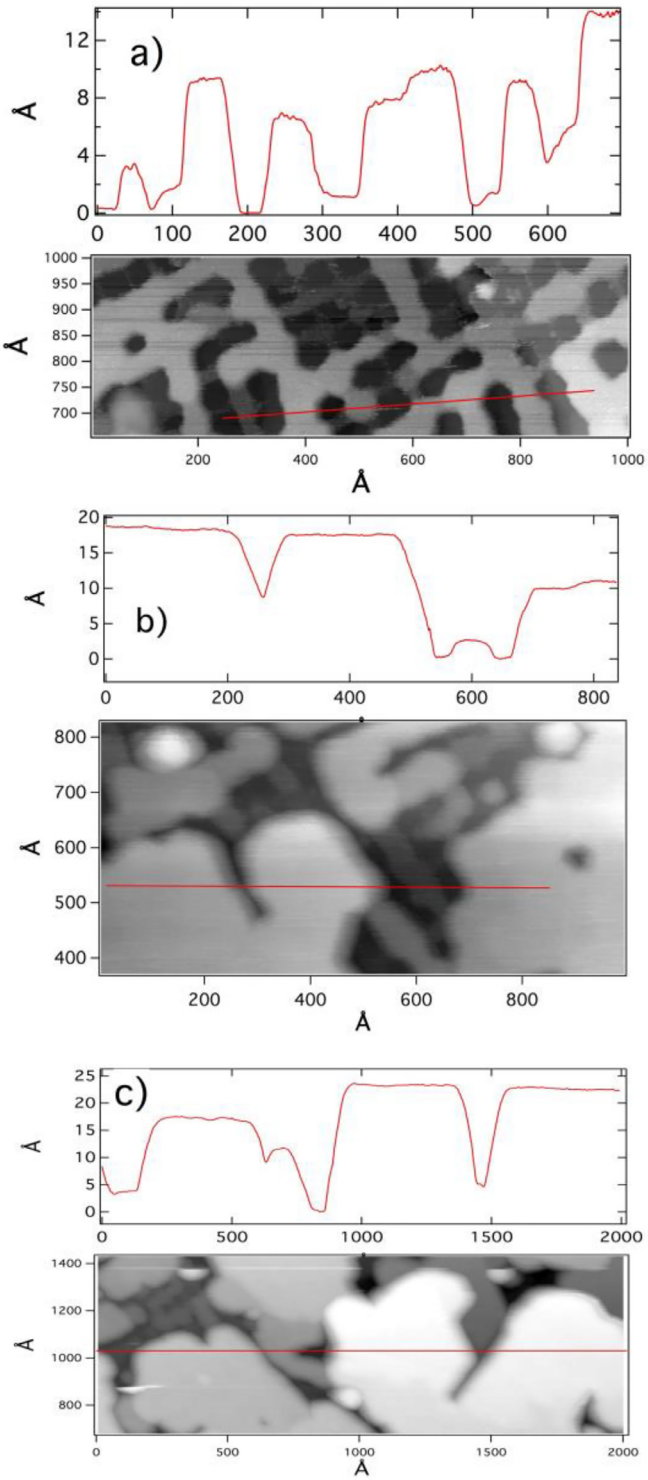

Fig. 3. Line profiles from STM images. (a) 1 ML. (b) 4 ML. (c) 8 ML.

of Ag islands observed especially for high Ag coverage may be induced by the surfactant effect of segregated N atoms, which we could not observe directly by STM images. The flat top of the islands at high coverage and the presence of a LEED pattern typical of Ag(111) surface would suggest uniformity also of the substrate, and this finding would be consistent with displacements of N atoms when Ag starts covering the N patches, or their segregation. Finally we remind that the Ag overlayer was not annealed and the film morphology is the result of the room temperature mobility of the Ag atoms. As a result of the high

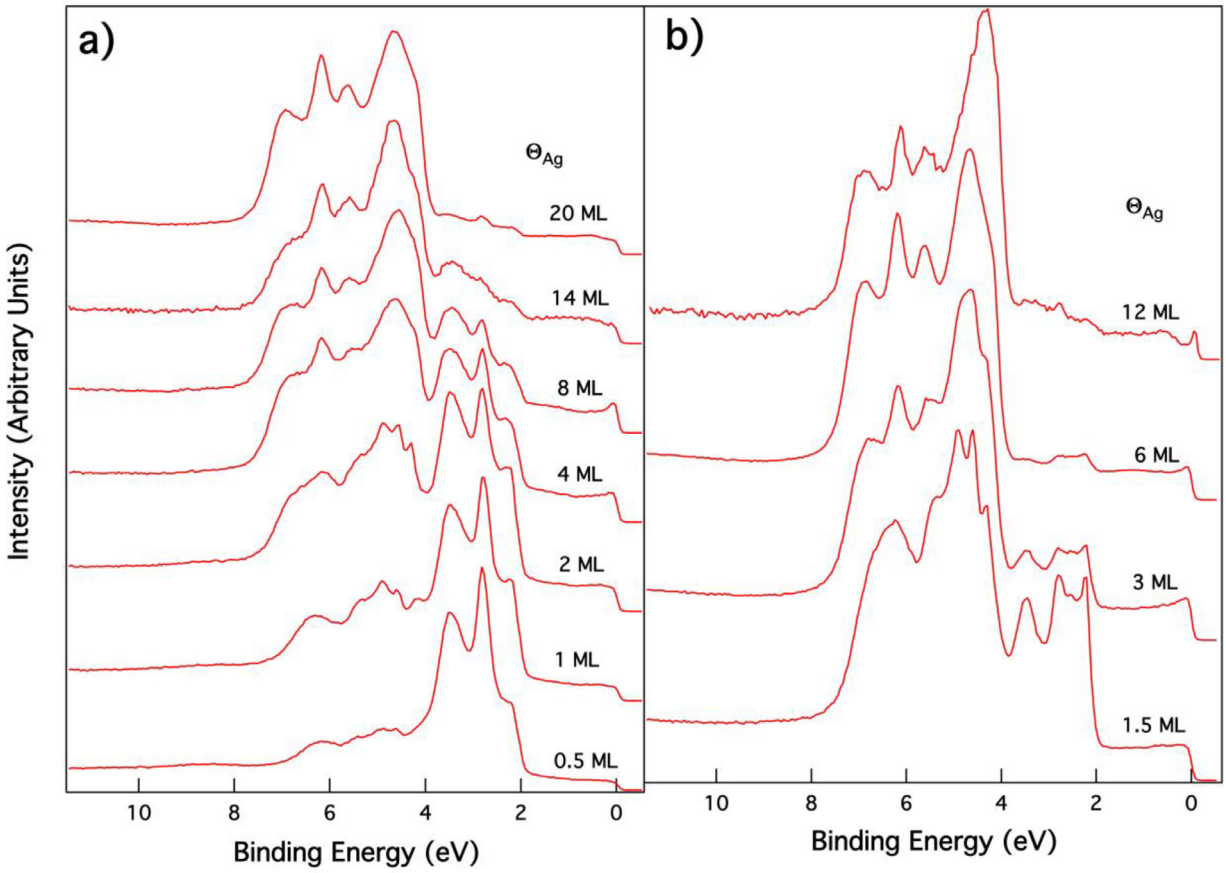

Fig. 4. Normal emission spectra integrated over an angle of 14° acquired at a photon energy $h\upsilon$ = 47.7 eV for a variable Ag coverage Θ_{Ag}. (a) Ag evaporated onto a 0.25 ML c(2 × 2)-N/Cu(001) surface. (b) Ag evaporated on a clean Cu(001) surface.

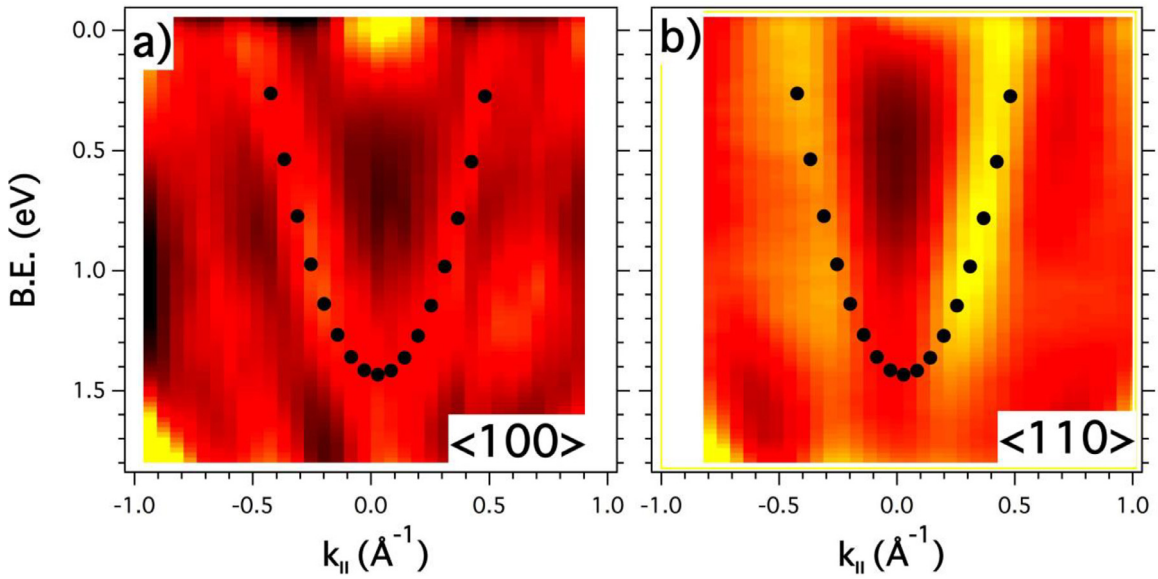

Fig. 5. ARPES data acquired on 4 ML of Ag deposited on 0.25 ML c(2 × 2)-N/Cu(001). Black dotted line: measured dispersion of the QW states. (a) ARPES along the ⟨100⟩ azimuth. (b) ARPES along the ⟨110⟩ azimuth. Photon energy hn = 47.7 eV. Note that the colour scale of Fig. 5a and 5b was compressed to increase the visibility of QW. (For interpretation of the references to colour in this figure legend, the reader is referred to the web version of this article.)

mobility, the Ag stripes and islands show an atomically flat top at all coverage studied.

3.2. Photoemission results

The (AR)PES experiments were carried out by varying the Ag coverage in the range between 0.5 ML and 20 ML. As observed by STM, in this range the morphology of the Ag overlayer evolves from the

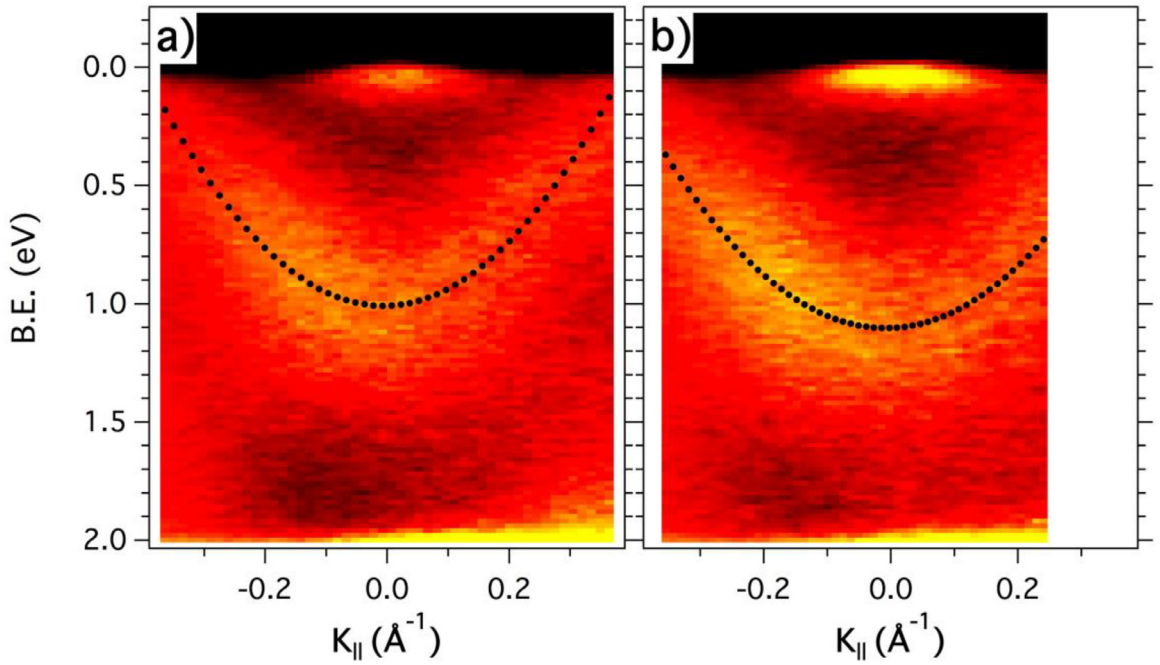

Fig. 6. ARPES data acquired on 8 ML of Ag deposited on 0.25 ML c(2 × 2)-N/Cu(001). Black dotted line: measured dispersion of the QW states. (a) ARPES along the ⟨100⟩ azimuth. (b) ARPES along the ⟨110⟩ azimuth. Photon energy hn = 47.7 eV. (For interpretation of the references to colour in this figure legend, the reader is referred to the web version of this article.)

predominant presence of stripes (0.5 ML ≤ Θ_{Ag} < 2 ML) to a 2-D island structure (Θ_{Ag} > 4ML).

Normal emission photoemission spectra (Fig. 4) shows that Cu 3d bands (around 2 eV-4 eV binding energy) are more persistent in Ag films grown c(2 × 2)-N/Cu(001) than in Ag films grown on clean Cu (001) at the same Ag grown quantity. This effect can be readily explained from STM data. In the former case in fact, there are regions of the surface covered by N-islands arrays, and Ag tends to be confined only on the clean Cu areas, so that a part of the surface tend to be "passivated" by the adsorbed N atoms, remaining uncovered. The spectrum taken at 20 ML on the N precovered surface is very similar to the one taken at 12 ML on clean Cu. This shows that at 20 ML thickness the Ag film covers the entire Cu surface and the growth proceeds as it would do on clean Cu. Note that the angular integration of the normal emission spectra shown in Fig. 4 is 14°. This explains the low visibility of QW states and of the Ag surface Schockley state, which is instead clearly visible in the angle resolved data (see below).

The photoemission data presented in this paper are also the first experimental evidence of the quantum size effect [4] in Ag nanostructured films formed onto the N-modified Cu(001) surface. QW of Ag films on Cu were observed for Ag grown on Cu(111) [39].

Fig. 5 reports ARPES data taken from 4 ML Ag grown on sub-saturated N-precovered Cu(001). The sub-saturation N pre-coverage was chosen to be 0.25 ML, corresponding to the N coverage giving rise to the STM images shown in Fig. 1(a) and (b), while the STM image corresponding to 4 ML Ag grown on N(0.25 ML)-Cu is shown in Fig. 2(d).

The photoemission data clearly shows the electron confinement effects in the form of QW states with parabolic dispersion in $k_{||}$. The coverage at which the QW states begins to be observed is 4 ML. The QW states are generally broad, which is an indication of non perfectly uniform thickness contributing to the confinement effect. They are more intense along the ⟨100⟩ azimuth, where also a second QW can be observed. This second QW is too broad for a safe assignment of its BE and its dispersion is not shown. The higher order QW can be observed also along the < 110 > azimuth but it is weaker. The different level of visibility of the QW states along the two azimuthal directions is attributed to differences in the background shape. The Ag(111) Schockley surface state is clearly visible and more intense near normal emission. At the nominal coverage of 4 ML, the STM images shows predominance of 2D structure in the form of very wide (tens of nanometers) islands 7–8 ML high, in agreement with the measured binding energies of the QWSs (1.5 eV and 2.6 eV for QW1 and QW2 respectively) corresponding to a 7–8 ML Ag film. Data acquired along the ⟨100⟩ and ⟨110⟩ azimuth, which lies at 45° relative to the stripes domains, show the same dispersion. We therefore conclude that the QW states are due to 2D confinement of electrons in the wide Ag islands that are predominant at 4 ML thickness, and not on the Ag stripes that coexist with the islands at 4 ML but are predominant at lower Ag coverage. The same conclusion clearly applies to QW states observed at higher coverage.

For an Ag coverage < 2 ML, where the stripe-shaped growth of Ag is predominant no QW state was observed despite the fact that the thickness of the Ag islands on a Cu(001) surface pre-covered with 0.25 ML of N can reach the height of 4 layers. Note that with 4 layers height it is very likely that the bottom of the QW dispersion curve (which lies at a binding energy of approximately 2.9 eV) is superimposed to the Cu 3d structure and cannot be observed. For a given order n in fact the binding energy of the QW decreases with the thickness [40,49]. The lack of QW in the stripe-shaped Ag overlayers can find several explanations, such as the average height of the islands is too small and irregular or the width of the islands is too irregular due to the faceting at the islands corners (from the STM images it can be noted that the Ag overlayer is very precisely confined by the N islands) and cause broadening of the QW states so that they are difficult to observe (see Fig. 2). Superposition of the Cu 3d band with the QW can be also another reason.

Fig. 6 shows the QW states observed at a coverage of 8 ML (see f) for the corresponding STM image], where the average thickness of the Ag islands is 10 ML, also in this case in agreement with the binding energies of the QWSs (1 eV and 2 eV for QW1 and QW2 respectively, with QW2 state hardly visible) corresponding to a 10 ML Ag film. The QW structure is still broad, which is again an indication of nonuniform thickness of the Ag layer. Also in this case the dispersion of the QW is the same along different azimuthal directions. ARPES data were also

acquired for Ag deposition on clean Cu(001), where the dispersion of the QW states is identical to the one shown on the N-modified surface.

4. Conclusions

We have studied the growth of Ag on the subsaturated C(2 × 2)-N/Cu(001) surface with an N precoverage of 0.25 ML. This N modified Cu (001) surface consists of about 50% striped domains of clean Cu(001) where the stripes run along the < 100 > azimuth and have a regular width. These clean Cu stripes are delimited by arrays of c(2 × 2)-N islands with a regular size that are separated by one line of atomic Cu. Up to a coverage of 1 ML in volume, the Ag overlayer growth is confined by the N islands onto the clean Cu islands. At a volume corresponding to 1 ML of Ag the growth starts to spill-over the N covered part of the surface and formation of 2D structures begins to occur at step edges. However the preferential Ag-on-Ag growth continues and the thickness of the islands grows more quickly than it would be if it were determined by the volume of deposited Ag. The structure consisting of mostly separated islands continues in fact up to a coverage of 8 ML where all the islands begin to coalesce to form a uniform film. The wide islands formed at coverages above 4 ML in volume (7–8 ML thickness) gives rise to QW states emission observed in ARPES. These QW states have been assigned to 2D confinement of electrons in wide islands, each of them behaving like a film. The measured binding energy of the QW states is consistent with the height of the islands as measured with STM.

Acknowledgements

Elettra infrastructure is acknowledged for providing access to synchrotron radiation.

References

[1] S.L. Silva, F.M. Leibsle, Surf. Sci 440 (1999) L835.
[2] R. Plass, J.A. Last, N.C. Bartelt, G.L. Kellogg, Nature 412 (2001) 875.
[3] S. Helveg, W.X. Li, N.C. Bartelt, S. Horch, E. Laegsgaard, B. Hammer, F. Besenbacher, Phys. Rev. Lett 98 (2007) 115501.
[4] M. Grundmann, Physica E (5) (2000) 167.
[5] H-Y Liu, B. Xu, Y-Q Wei, D. Ding, J.-J. Qian, Q. Han, J.-B. Liang, Z.-G. Wang, Appl. Phys. Lett 79 (2001) 2868.
[6] H. Eisele, A. Lenz, R. Heitz, R. Timm, M. Dähne, Y. Temko, T. Suzuki, K. Jacobi, J. Appl. Phys 104 (2008) 124301.
[7] T. Ohta, A. Bostwick, T. Seyller, K. Horn, E. Rotenberg, Science 313 (2006) 951.
[8] P.W. Sutter, J.-I. Flege, E.A. Sutter, Nature Mat 7 (2008) 406.
[9] J. Campos-Delgado, J.M. Romo-Herrera, X. Jia, D.A. Cullen, H. Muramatsu, Y.A. Kim, T Hayashi, Z Ren, D.J. Smith, Y. Okuno, T. Ohba, H. Kanoh, K. Kaneko, M. Endo, H. Terrones, M.S. Dresselhaus, M. Terrones, Nanolett 8 (2008) 2773.
[10] Z. Chen, W. Zhang, C.-A. Palma, et al., J. Am. Chem. Soc. 138 (2016) 15488.
[11] S. D'Addato, V. Grillo, S. Altieri, S. Frabboni, S. Valeri, Appl. Surf. Sci 260 (2012) 13.
[12] C. Carbone, S. Gardonio, P. Moras, et al., Adv. Func. Mat. 21 (2011) 1212.
[13] F.M. Leibsle, C.F.J. Flipse, A.W. Robinson, Phys. Rev 47 (B) (1993) 15865.
[14] F.M. Leibsle, S.S. Dhesi, S.D. Barrett, A.W. Robinson, Surf. Sci 317 (1994) 309.
[15] C. Cohen, H. Ellmer, J.M. Guigner, A. L'Hoir, G. Prévot, D. Schmaus, M. Sotto, Surf. Sci 490 (2001) 336.
[16] B. Croset, Y. Girard, G. Prévot, M. Sotto, Y. Garreau, R. Pinchaux, M. Sauvage-Simkin, Phys, Rev. Lett 88 (2002) 056103.
[17] M. Sotto, S. Gauthier, F. Pourmir, S. Rousset, J. Klein, Surf. Sci 371 (1997) 658.
[18] M. Sotto, B. Croset, Surf. Sci 461 (2000) 78.
[19] S. D'Addato, F. Borgatti, R. Felici, P. Finetti, Surf. Sci 606 (2012) 813.
[20] M. Yamada, N. Kawamura, K. Nakatsuji, F. Komori, e-J. Surf. Sci. Nanotech 14 (2016) 43.
[21] T. Hattori, M. Yamada, F. Komori, Surf. Sci 655 (2017) 1.
[22] T. Parker, L. Wilson, N. Condon, F. Leibsle, Phys. Rev 56 (B) (1997) 6458.
[23] Y. Matsumoto, K.-I. Tanaka, Jpn. J. Appl. Phys 37 (1998) L154.
[24] K. Mukai Y. Matsumoto, K. Tanaka, F. Komori, Surf. Sci 450 (2000) 44.
[25] S.L. Silva, C.R. Jenkins, S.M. York, F.M. Leibsle, Appl. Phys. Lett 76 (2000) 1128.
[26] G. Prévot, H Guesmi, B. Croset, Surf. Sci 601 (2007) 2017.
[27] K. Nakatsuji, Y. Yoshimoto, D. Sekiba, S. Doi, T. Iimori, K. Yagyu, Y. Takagi, S.-Y. Ohno, H. Miyaoka M. Yamada, F. Komori, K. Amemiya, D. Matsumura, T. Ohta, Phys. Rev B (77) (2008) 235436.
[28] S. D'Addato, C. Binns, P. Finetti, Surf. Sci 442 (1999) 74.
[29] P. Finetti, F. Borgatti, R. Felici, R. Gunnella, S. D'Addato, Appl. Surf. Sci 212 (2003) 85.
[30] S. D'Addato, R. Gunnella, F. Borgatti, R. Felici, P. Finetti, Surf. Sci 601 (2007) 329.
[31] K.-D. Lee, T. Iimori, F. Komori, Surf. Sci 860 (2000) 454–456.
[32] P. Finetti, V.R. Dhanak, C. Binns, L.W. Edmonds, S.H. Baker, S. D'Addato, J. Electron Spectrosc, Rel. Phenom 114 (2001) 251.
[33] Y. Takagi, K. Isami, I. Yamamoto, T. Nakagawa, T. Yokoyama, Phys. Rev 81 (B) (2010) 035422.
[34] S.M. York, F.M. Leibsle, Appl. Phys. Lett 78 (2001) 2763.
[35] P. Sprunger, E. Laegsgaard, F. Besenbacher, Phys. Rev 54 (B) (1996) 8163.
[36] J.G. Tobin, S.W. Robey, D.A. Shirley, Phys. Rev 33 (B) (1986) 2270.
[37] J.G. Tobin, S.W. Robey, L.E. Klebanoff, D.A. Shirley, Phys. Rev 35 (B) (1987) 9056.
[38] M.A. Mueller, A. Samsavar, T. Miller, T.-C. Chiang, Phys. Rev 40 (B) (1989) 5845.
[39] M.A. Mueller, T. Miller, T.-C. Chiang, Phys. Rev 41 (B) (1990) 5214.
[40] J.J. Paggel, T. Miller, T.-C. Chiang, Science 283 (1999) 170.
[41] T.-C. Chiang, Surf. Sci. Rep 39 (2000) 181.
[42] D.A. Evans, M. Alonso, R. Cimino, K. Horn, Phys. Rev. Lett 70 (1993) 3483.
[43] P. Moras, D. Topwal, et al., Phys. Rev 80 (B) (2009) 205418.
[44] P. Moras, G. Bihlmayer, E. Vescovo, P.M. Sheverdyaeva, M. Papagno, L. Ferrari, C. Carbone, J. Phys, Condensed Matter 29 (2017) 495806.
[45] P.W. Palmberg, T.N. Rhodin, J. Chem. Phys 49 (1968) 134.
[46] J. Hayoz, D. Naumović, R. Fasel, P. Aebi, L.Schlapbach, Surf. Sci 373 (1997) 153.
[47] H. Sheng, E. Ma, Phys. Rev 61 (B) (2000) 9979.
[48] D. Sekiba, S. Doi, K. Nakatsuji, F. Komori, Surf. Sci 590 (2005) 138.
[49] I. Matsuda, H.W Yeom, T. Tanikawa, K. Tono, T. Nagao, S. Hasegawa, T. Ohta, Phys. Rev 63 (B) (2001) 125325.